Available online at www.sciencedirect.com
SCIENCE DIRECT®
Journal of Sound and Vibration 276 (2004) 181–193
JOURNAL OF SOUND AND VIBRATION
www.elsevier.com/locate/jsvi

Three-dimensional hierarchical finite element free vibration analysis of annular sector plates

A. Houmat*

Department of Mechanical Engineering, Faculty of Engineering, University of Tlemcen, Tlemcen 13000, Algeria

Received 27 March 2003; accepted 24 July 2003

Abstract

An annular sector solid hierarchical finite element is presented and applied to three-dimensional free vibration analysis of annular sector plates. The element's displacements are expressed in terms of a fixed number of linear polynomial shape functions plus a variable number of shape functions which are forms of the shifted Legendre orthogonal polynomial. The linear polynomial shape functions are used to describe the element's nodal displacements and the higher order shape functions are used to provide additional freedom to the edges, faces, and interior of the element. Results of frequency calculations are found for annular sector plates with two straight edges simply supported like a diaphragm condition and comparisons are made with those obtained by the finite prism method. The manner of convergence of the solution as a function of the numbers of hierarchical modes is also investigated. Furthermore, contributions to original three-dimensional frequencies are made for annular sector plates with other boundary conditions along the two straight edges.

1. Introduction

Approximate plate theories neglect some or all of complicating effects such as shear deformation, rotary inertia, extension of the normal to the middle surface, and other kinematic effects. To take into account all these effects, a three-dimensional formulation is required. Mizusawa [1] presented a finite prism method (FPM) for three-dimensional free vibration analysis of annular sector plates. A major drawback of this method is that its use is limited to annular sector plates with two opposite straight edges simply supported like a diaphragm condition.

The aim of this paper is three-fold: to introduce and assess the applicability of a three-dimensional hierarchical finite element method; to compare the results with those obtained by the

*Tel.: +213-43-20-0192; fax: +213-43-28-5685.
E-mail address: a_houmat@mail.univ-tlemcen.dz (A. Houmat).

0022-460X/$ - see front matter © 2003 Elsevier Ltd. All rights reserved.
doi:10.1016/j.jsv.2003.07.020

FPM for a number of annular sector plates with two opposite straight edges simply supported like a diaphragm condition; and to contribute to original three-dimensional frequencies for a number of annular sector plates with other boundary conditions along the two opposite straight edges.

The displacements in the annular sector solid hierarchical finite element of this paper are described by a fixed number of linear polynomial shape functions plus a variable number of shape functions which are forms of the shifted Legendre orthogonal polynomial. The linear polynomial shape functions are used to describe the element's nodal displacements and the higher order polynomial shape functions are used to provide additional freedom to the twelve edges, six faces, and interior of the element. The principle of virtual displacements is used to develop the equations of motion. The resulting equations form a generalized eigenvalue problem which is solved to yield the frequencies. The results can be obtained to any desired degree of accuracy simply by increasing the numbers of hierarchical modes.

2. Formulation

2.1. The shape functions

The shape functions will be derived on the basis of a one-dimensional hierarchical finite element. The origin of the non-dimensional co-ordinate ξ $(= x/a)$ is the left end of the element (Fig. 1). For C^0 continuous problems the first two linear shape functions used in the conventional finite element method are retained. The higher order C^0shape functions vanish at each end of the element. Thus, these shape functions are used to describe the displacement function in the interior of the element.

The higher order shape functions can be selected from a variety of polynomials provided the set is complete. The set of hierarchical shape functions of this paper is generated by using the following recursive formula for the shifted Legendre orthogonal polynomial $P_i^*(\xi)$ [2]:

$$P_{i+1}^*(\xi) = \frac{1}{i+1}[(-2i-1+(4i+2)\xi)P_i^*(\xi) - iP_{i-1}^*(\xi)], \quad i = 1, 2, \ldots \tag{1}$$

with

$$P_0^*(\xi) = 1, \tag{2}$$

$$P_1^*(\xi) = 2\xi - 1. \tag{3}$$

The C^0 shape functions are expressed as

$$g_1(\xi) = 1 - \xi, \tag{4}$$

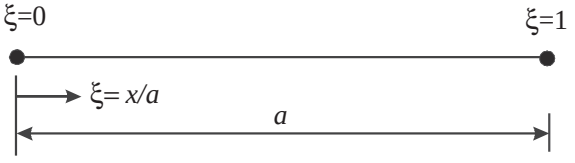

Fig. 1. Hierarchical finite element co-ordinates.

$$g_2(\xi) = \xi, \tag{5}$$

$$g_{i+2}(\xi) = \int_0^{\xi} \mathrm{P}_i^*(\zeta)\,\mathrm{d}\zeta \quad \text{for } i \geqslant 1. \tag{6}$$

The first 12 hierarchical C^0 shape functions $g_i(\xi)$ $(i = 1, 2, ..., 12)$ are quoted explicitly in Table 1.

2.2. The annular sector plate equations of motion

An annular sector solid hierarchical finite element is shown in Fig. 2 (a list of nomenclature is given in Appendix B). The circular cylindrical and the non-dimensional co-ordinates are related by

$$\xi = \frac{r-a}{b-a}, \tag{7}$$

$$\eta = \frac{\theta}{\phi}, \tag{8}$$

$$\zeta = \frac{2z}{h}. \tag{9}$$

The displacement vector is

$$\mathbf{u} = \begin{Bmatrix} u \\ v \\ w \end{Bmatrix}. \tag{10}$$

Table 1
The first 12 hierarchical C^0 shape functions

i	$g_i(\xi)$
1	$1-\xi$
2	ξ
3	$\xi^2-\xi$
4	$2\xi^3-3\xi^2+\xi$
5	$5\xi^4-10\xi^3+6\xi^2-\xi$
6	$14\xi^5-35\xi^4+30\xi^3-10\xi^2+\xi$
7	$42\xi^6-126\xi^5+140\xi^4-70\xi^3+15\xi^2-\xi$
8	$132\xi^7-462\xi^6+630\xi^5-420\xi^4+140\xi^3-21\xi^2+\xi$
9	$429\xi^8-1716\xi^7+2772\xi^6-2310\xi^5+1050\xi^4-252\xi^3+28\xi^2-\xi$
10	$1430\xi^9-6435\xi^8+12012\xi^7-12012\xi^6+6930\xi^5-2310\xi^4+420\xi^3-36\xi^2+\xi$
11	$4862\xi^{10}-24310\xi^9+51480\xi^8-60060\xi^7+42042\xi^6-18018\xi^5+4620\xi^4-660\xi^3+45\xi^2-\xi$
12	$16796\xi^{11}-92378\xi^{10}+218790\xi^9-291720\xi^8+240240\xi^7-126126\xi^6+42042\xi^5-8580\xi^4+990\xi^3-55\xi^2+\xi$

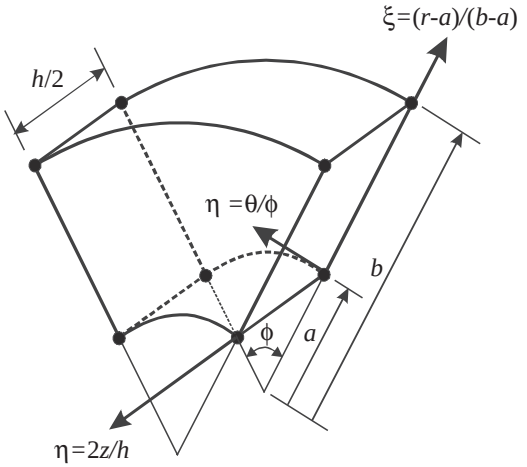

Fig. 2. Annular sector solid hierarchical finite element.

The strain vector is

$$\boldsymbol{\varepsilon} = \begin{Bmatrix} \varepsilon_{rr} \\ \varepsilon_{\theta\theta} \\ \varepsilon_{zz} \\ \gamma_{r\theta} \\ \gamma_{rz} \\ \gamma_{\theta z} \end{Bmatrix}. \tag{11}$$

The strain–displacement relation is

$$\boldsymbol{\varepsilon} = \mathbf{d}\mathbf{u}, \tag{12}$$

where

$$\mathbf{d} = \begin{bmatrix} \dfrac{1}{(b-a)}\dfrac{\partial}{\partial\xi} & 0 & 0 \\ \dfrac{1}{(b-a)(\xi + a/(b-a))} & \dfrac{1}{\phi(b-a)(\xi + a/(b-a))}\dfrac{\partial}{\partial\eta} & 0 \\ 0 & 0 & \dfrac{2}{h}\dfrac{\partial}{\partial\zeta} \\ \dfrac{1}{\phi(b-a)\left(\xi + a/(b-a)\right)}\dfrac{\partial}{\partial\eta} & \dfrac{1}{(b-a)}\dfrac{\partial}{\partial\xi} - \dfrac{1}{(b-a)(\xi + a/(b-a))} & 0 \\ \dfrac{2}{h}\dfrac{\partial}{\partial\zeta} & 0 & \dfrac{1}{(b-a)}\dfrac{\partial}{\partial\xi} \\ 0 & \dfrac{2}{h}\dfrac{\partial}{\partial\zeta} & \dfrac{1}{\phi(b-a)(\xi + a/(b-a))}\dfrac{\partial}{\partial\eta} \end{bmatrix}. \tag{13}$$

The displacement vector can be written

$$\mathbf{u} = \mathbf{Nq} = [\mathbf{N}_1\mathbf{N}_2 \ldots \mathbf{N}_\alpha \ldots \mathbf{N}_{LMN}]\mathbf{q}, \tag{14}$$

where

$$\mathbf{N}_\alpha = \begin{bmatrix} g_i(\xi)g_j(\eta)g_k(\zeta) & 0 & 0 \\ 0 & g_i(\xi)g_j(\eta)g_k(\zeta) & 0 \\ 0 & 0 & g_i(\xi)g_j(\eta)g_k(\zeta) \end{bmatrix}. \tag{15}$$

The strain–displacement relation can be written

$$\boldsymbol{\varepsilon} = \mathbf{dNq} = \mathbf{Bq} = [\mathbf{B}_1\mathbf{B}_2 \ldots \mathbf{B}_\alpha \ldots \mathbf{B}_{LMN}]\mathbf{q}, \tag{16}$$

where

$$\mathbf{B}_\alpha = \mathbf{dN}_\alpha. \tag{17}$$

Let

$$\mathbf{N}_\beta = \begin{bmatrix} g_l(\xi)g_m(\eta)g_n(\zeta) & 0 & 0 \\ 0 & g_l(\xi)g_m(\eta)g_n(\zeta) & 0 \\ 0 & 0 & g_l(\xi)g_m(\eta)g_n(\zeta) \end{bmatrix}. \tag{18}$$

Then

$$\mathbf{B}_\beta = \mathbf{dN}_\beta. \tag{19}$$

The indices are defined as

$$i, l = 1, 2, \ldots, L, \tag{20}$$

$$j, m = 1, 2, \ldots, M, \tag{21}$$

$$k, n = 1, 2, \ldots, N, \tag{22}$$

$$\alpha = k + (j-1)N + (i-1)MN, \tag{23}$$

$$\beta = n + (m-1)N + (l-1)MN. \tag{24}$$

The principle of virtual displacements can be applied to yield the following equations of motion for free vibration:

$$\sum_{\alpha=1}^{LMN} (\mathbf{K}_{\alpha,\beta} - \omega^2 \mathbf{M}_{\alpha,\beta})\, \mathbf{q}_\beta = \mathbf{0}, \quad \beta = 1, 2, \ldots, LMN. \tag{25}$$

The element stiffness matrix can be evaluated as

$$\begin{aligned} \mathbf{K}_{\alpha,\beta} &= \frac{1}{2}(b-a)^2 \phi h \int_0^1 \int_0^1 \int_0^1 \mathbf{B}_\alpha^{\mathrm{T}} \mathbf{D} \mathbf{B}_\beta \left(\xi + \frac{a}{b-a}\right) \mathrm{d}\xi\, \mathrm{d}\eta\, \mathrm{d}\zeta \\ &= \begin{bmatrix} K_{3\alpha-2,3\beta-2} & K_{3\alpha-2,3\beta-1} & K_{3\alpha-2,3\beta} \\ K_{3\alpha-1,3\beta-2} & K_{3\alpha-1,3\beta-1} & K_{3\alpha-1,3\beta} \\ K_{3\alpha,3\beta-2} & K_{3\alpha,3\beta-1} & K_{3\alpha,3\beta} \end{bmatrix}, \end{aligned} \tag{26}$$

where

$$\mathbf{D} = \frac{E}{(1+v)(1-2v)} \begin{bmatrix} 1-v & v & v & 0 & 0 & 0 \\ v & 1-v & v & 0 & 0 & 0 \\ v & v & 1-v & 0 & 0 & 0 \\ 0 & 0 & 0 & \dfrac{1-2v}{2} & 0 & 0 \\ 0 & 0 & 0 & 0 & \dfrac{1-2v}{2} & 0 \\ 0 & 0 & 0 & 0 & 0 & \dfrac{1-2v}{2} \end{bmatrix}. \tag{27}$$

The element mass matrix can be evaluated as

$$\begin{aligned} \mathbf{M}_{\alpha,\beta} &= \frac{1}{2}\rho(b-a)^2\phi h \int_0^1 \int_0^1 \int_0^1 \mathbf{N}_\alpha^{\mathrm{T}} \mathbf{N}_\beta \left(\xi + \frac{a}{b-a}\right) \mathrm{d}\xi \, \mathrm{d}\eta \, \mathrm{d}\zeta \\ &= \begin{bmatrix} M_{3\alpha-2,3\beta-2} & M_{3\alpha-2,3\beta-1} & M_{3\alpha-2,3\beta} \\ M_{3\alpha-1,3\beta-2} & M_{3\alpha-1,3\beta-1} & M_{3\alpha-1,3\beta} \\ M_{3\alpha,3\beta-2} & M_{3\alpha,3\beta-1} & M_{3\alpha,3\beta} \end{bmatrix}. \end{aligned} \tag{28}$$

The coefficients of the element stiffness and mass matrices are given in Appendix A. They are expressed in terms of the following integrals:

$$A_{j,m}^{p,q} = \int_0^1 \frac{\mathrm{d}^p g_j}{\mathrm{d}\eta^p} \frac{\mathrm{d}^q g_m}{\mathrm{d}\eta^q} \mathrm{d}\eta, \tag{29}$$

$$A_{k,n}^{p,q} = \int_0^1 \frac{\mathrm{d}^p g_k}{\mathrm{d}\zeta^p} \frac{\mathrm{d}^q g_n}{\mathrm{d}\zeta^q} \mathrm{d}\zeta, \tag{30}$$

$$B_{i,l}^{p,q} = \int_0^1 \left(\xi + \frac{a}{b-a}\right) \frac{\mathrm{d}^p g_i}{\mathrm{d}\xi^p} \frac{\mathrm{d}^q g_l}{\mathrm{d}\xi^q} \mathrm{d}\xi, \tag{31}$$

$$C_{i,l}^{p,q} = \int_0^1 \frac{1}{(\xi + a/(b-a))} \frac{\mathrm{d}^p g_i}{\mathrm{d}\xi^p} \frac{\mathrm{d}^q g_l}{\mathrm{d}\xi^q} \mathrm{d}\xi, \tag{32}$$

where p and q denote the order of the derivatives (p, $q = 0$, 1).

The above integrals can be calculated exactly by using symbolic computing which is available through a number of commercial packages.

Particular displacement boundary conditions can be assigned to the element's eight nodes, twelve edges, and six faces and it is possible to accommodate various combinations of nodal, edge, and face boundary conditions in the analysis. The resultant equations can be solved as a generalized eigenvalue problem to yield the frequencies.

3. Results

Natural frequencies of annular sector plates are calculated to illustrate the convergence and accuracy of the hierarchical finite element method (HFEM). The straight and circumferential

edges may have arbitrary boundary conditions. Symbolism is used to define the boundary conditions along the four edges. For example, the symbolism F-C-S-S indicates that the edges $r = a$, $r = b$, $\theta = 0$, and $\theta = \phi$ are free, clamped, simply supported, and simply supported, respectively. A non-dimensional frequency Ω is used in the calculations. A value of ν of 0.3 will be used in all examples. Results were first obtained for an annular sector S-S-S-S plate ($a/b = 0.5$, $\phi = 60^\circ$) with $h/b = 0.2$ (thick) and 0.4 (very thick).

To see the manner of convergence of the hierarchical finite element method, half of the annular sector plate above the middle surface is idealized as one annular sector solid hierarchical finite element and the numbers of hierarchical modes L, M, and N are varied. An equal number of hierarchical modes is utilized in the r and θ directions and half as many hierarchical modes are used in the z direction. For flexural vibration, the displacement boundary conditions on the middle surface must be $u(r, \theta, 0) = v(r, \theta, 0) = 0$. Results for the 5 lowest modes are shown in Table 2. It is clearly shown that the frequencies are rapidly convergent from above as the numbers of hierarchical modes are increased. The higher order hierarchical finite element ($N = M = 2L = 12$) will be used in the next examples.

To demonstrate the accuracy of the hierarchical finite element method, non-dimensional frequencies Ω for the 5 lowest modes of annular sector S-S-S-S, C-C-S-S, and F-F-S-S plates ($a/b = 0.5$) are compared with those calculated by the FPM [1] in Tables 3–5. Values of ϕ of 30° and 60° and those of h/b of 0.005, 0.1, 0.3, and 0.5 are used. The values of h/b were chosen to encompass extremes from very thin to very thick plates. It is clearly shown that most of the hierarchical finite element results are the lower-bounds of the finite prism ones and are therefore more accurate. The discrepancies between the two solutions increase with increasing mode number or thickness ratio.

Additional applications are to annular sector S-S-C-C, C-C-C-C, and F-F-C-C plates. It appears that no three-dimensional frequencies are reported in the literature for these examples. Thus, new three-dimensional frequency values are provided which may be of interest to other investigators. Non-dimensional frequencies Ω for the 6 lowest modes are shown in Tables 6–8.

Table 2
Convergence of the non-dimensional frequencies Ω for the 5 lowest modes of annular sector S-S-S-S plates ($a/b = 0.5$, $\phi = 60^\circ$, $\nu = 0.3$)

h/b	L,M,N	Mode no.				
		1	2	3	4	5
0.2	4,4,2	2.718	4.685	6.977	8.211	11.018
	6,6,3	2.576	4.153	6.051	6.627	7.226
	8,8,4	2.572	4.137	6.015	6.115	7.174
	10,10,5	2.571	4.137	6.014	6.101	7.173
	12,12,6	2.571	4.137	6.014	6.101	7.173
0.4	4,4,2	3.725	5.742	5.908	6.686	7.240
	6,6,3	3.538	5.269	5.457	6.295	6.542
	8,8,4	3.520	5.224	5.440	6.281	6.522
	10,10,5	3.519	5.222	5.440	6.281	6.522
	12,12,6	3.519	5.222	5.440	6.281	6.522

Table 3
Comparison of the non-dimensional frequencies Ω for the 5 lowest modes of annular sector S-S-S-S plates ($a/b = 0.5$, $v = 0.3$)

h/b	ϕ (deg)	Method	Mode no.				
			1	2	3	4	5
0.005	30	HFEM	0.156	0.346	0.421	0.645	0.663
		FPM	0.156	0.346	0.420	0.646	0.662
	60	HFEM	0.085	0.156	0.266	0.271	0.346
		FPM	0.085	0.156	0.267	0.271	0.346
0.1	30	HFEM	2.696	5.243	6.128	8.464	8.639
		FPM	2.724	5.316	6.520	8.660	8.846
	60	HFEM	1.549	2.696	4.236	4.301	5.243
		FPM	1.557	2.724	4.278	4.368	5.318
0.3	30	HFEM	4.845	7.609	7.803	7.927	8.905
		FPM	4.922	7.666	8.228	9.130	9.378
	60	HFEM	3.166	4.845	6.756	6.853	6.929
		FPM	3.162	4.922	6.476	7.016	7.358
0.5	30	HFEM	5.438	5.559	5.834	8.213	8.452
		FPM	5.400	5.846	6.184	8.176	8.340
	60	HFEM	3.735	4.595	5.438	5.559	5.834
		FPM	3.638	4.566	5.356	5.400	5.846

Values of ϕ of 30°, 60°, and 90° and those of h/b of 0.005, 0.1, 0.3, and 0.5 are used. In all cases a value of a/b of 0.5 is used. The non-dimensional frequencies in Tables 6–8 can serve to validate other methods and finite element models.

4. Conclusion

A annular sector solid hierarchical finite element has been presented and applied to three-dimensional free vibration analysis of annular sector plates. The element's displacements are expressed in terms of a fixed number of linear polynomial shape functions plus a variable number of shape functions which are forms of the shifted Legendre orthogonal polynomial. To demonstrate the method, non-dimensional frequencies of annular sector plates with two straight edges simply supported like a diaphragm condition have been reported. Rapid convergence from above was found to occur as the numbers of hierarchical modes increased and excellent convergent results were obtained with the use of very few hierarchical modes. One main advantage of the HFEM over the finite prism method is that its use is not limited to annular sector plates with two straight edges simply supported. By using reasonable numbers of hierarchical

Table 4
Comparison of the non-dimensional frequencies Ω for the 5 lowest modes of annular sector C-C-S-S plates ($a/b = 0.5$, $v = 0.3$)

h/b	ϕ (deg)	Method	Mode no.				
			1	2	3	4	5
0.005	30	HFEM	0.206	0.456	0.463	0.737	0.821
		FPM	0.206	0.458	0.463	0.739	0.828
	60	HFEM	0.150	0.206	0.312	0.393	0.456
		FPM	0.151	0.206	0.312	0.396	0.458
0.1	30	HFEM	3.180	5.911	6.372	8.903	9.085
		FPM	3.248	6.092	6.538	9.180	9.404
	60	HFEM	2.363	3.180	4.614	5.168	5.911
		FPM	2.420	3.250	4.720	5.336	6.092
0.3	30	HFEM	5.044	7.609	8.020	8.968	9.769
		FPM	5.240	8.318	9.370	10.310	11.288
	60	HFEM	3.687	5.044	6.876	6.947	7.609
		FPM	3.846	5.240	7.110	7.360	8.320
0.5	30	HFEM	5.541	5.559	8.069	8.654	8.746
		FPM	5.768	8.290	9.090	9.752	9.786
	60	HFEM	4.026	5.541	5.559	6.646	7.273
		FPM	4.184	5.768	6.952	7.500	7.814

modes, the HFEM was found to yield a much higher accuracy than that of the finite prism method. Finally, contributions to original three-dimensional frequencies were made for a number of annular sector plates with other boundary conditions along the two straight edges. The tabulated non-dimensional frequencies can serve as a basis of comparison for other methods and finite element models.

Appendix A. Coefficients of $\mathbf{K}_{\alpha,\beta}$ and $\mathbf{M}_{\alpha,\beta}$

$$K_{3\alpha-2,3\beta-2} = \frac{E\phi h}{2(1+v)(1-2v)}\left[(1-v)B^{1,1}_{i,l}A^{0,0}_{j,m}A^{0,0}_{k,n} + \frac{(1-2v)}{2\phi^2}C^{0,0}_{i,l}A^{1,1}_{j,m}A^{0,0}_{k,n} + v(A^{1,0}_{i,l}A^{0,0}_{j,m}A^{0,0}_{k,n} + A^{0,1}_{i,l}A^{0,0}_{j,m}A^{0,0}_{k,n}) + \frac{2(1-2v)(b-a)^2}{h^2} \times B^{0,0}_{i,l}A^{0,0}_{j,m}A^{1,1}_{k,n} + (1-v)C^{0,0}_{i,l}A^{0,0}_{j,m}A^{0,0}_{k,n}\right], \quad \text{(A.1)}$$

Table 5
Comparison of the non-dimensional frequencies Ω for the 5 lowest modes of annular sector F-F-S-S plates ($a/b = 0.5$, $v = 0.3$)

h/b	ϕ (deg)	Method	Mode no.				
			1	2	3	4	5
0.005	30	HFEM	0.071	0.175	0.266	0.305	0.496
		FPM	0.071	0.175	0.266	0.305	0.496
	60	HFEM	0.017	0.071	0.072	0.154	0.175
		FPM	0.017	0.071	0.072	0.154	0.175
0.1	30	HFEM	1.304	2.929	4.180	4.617	6.883
		FPM	1.313	2.968	3.870	4.256	5.888
	60	HFEM	0.335	1.286	1.304	2.626	2.929
		FPM	0.336	1.298	1.314	1.393	2.662
0.3	30	HFEM	2.750	5.024	6.494	6.656	6.868
		FPM	2.824	3.868	6.104	6.944	7.188
	60	HFEM	0.863	2.565	2.750	4.715	5.024
		FPM	0.742	1.394	2.826	3.280	3.556
0.5	30	HFEM	3.309	3.897	5.142	5.748	6.333
		FPM	3.432	3.870	5.360	6.010	6.278
	60	HFEM	1.175	2.792	3.309	3.897	4.933
		FPM	1.202	1.398	3.432	3.532	3.872

$$K_{3\alpha-2,3\beta-1} = \frac{Eh}{2(1+v)(1-2v)}\Big[vA_{i,l}^{1,0}A_{j,m}^{0,1}A_{k,n}^{0,0} + (1-2v)A_{i,l}^{0,1}A_{j,m}^{1,0}A_{k,n}^{0,0} - (1-2v)C_{i,l}^{0,0}A_{j,m}^{1,0}A_{k,n}^{0,0} + (1-v)C_{i,l}^{0,0}A_{j,m}^{0,1}A_{k,n}^{0,0}\Big], \tag{A.2}$$

$$K_{3\alpha-2,3\beta} = \frac{E\phi}{(1+v)(1-2v)}\Big[v(b-a)B_{i,l}^{1,0}A_{j,m}^{0,0}A_{k,n}^{0,1} + (1-2v)(b-a) \times B_{i,l}^{0,1}A_{j,m}^{0,0}A_{k,n}^{1,0} + v(b-a)A_{i,l}^{0,0}A_{j,m}^{0,0}A_{k,n}^{0,1}\Big], \tag{A.3}$$

$$K_{3\alpha-1,3\beta-2} = \frac{Eh}{2(1+v)(1-2v)}\Big[vA_{i,l}^{0,1}A_{j,m}^{1,0}A_{k,n}^{0,0} + (1-2v)A_{i,l}^{1,0}A_{j,m}^{0,1}A_{k,n}^{0,0} -(1-2v)C_{i,l}^{0,0}A_{j,m}^{0,1}A_{k,n}^{0,0} + (1-v)C_{i,l}^{0,0}A_{j,m}^{1,0}A_{k,n}^{0,0}\Big], \tag{A.4}$$

Table 6
Non-dimensional frequencies Ω for the 6 lowest modes of annular sector S-S-C-C plates ($a/b = 0.5$, $v = 0.3$)

h/b	ϕ (deg)	Mode no.					
		1	2	3	4	5	6
0.005	30	0.251	0.429	0.584	0.705	0.851	1.040
	60	0.102	0.199	0.276	0.333	0.381	0.500
	90	0.077	0.120	0.184	0.254	0.265	0.298
0.1	30	3.615	5.727	6.985	8.666	9.277	10.655
	60	1.779	3.137	4.314	4.791	5.467	6.582
	90	1.396	2.067	2.988	4.059	4.066	4.588
0.3	30	5.218	8.045	8.250	8.944	10.044	10.735
	60	3.311	5.007	6.782	6.917	7.128	7.766
	90	2.843	3.770	4.956	6.252	6.531	6.835
0.5	30	5.567	6.429	8.493	8.542	9.193	9.512
	60	3.785	4.834	5.495	5.782	7.138	7.247
	90	3.349	4.282	4.459	5.034	5.482	5.861

Table 7
Non-dimensional frequencies Ω for the 6 lowest modes of annular sector C-C-C-C plates ($a/b = 0.5$, $v = 0.3$)

h/b	ϕ (deg)	Mode no.					
		1	2	3	4	5	6
0.005	30	0.292	0.519	0.633	0.866	0.916	1.104
	60	0.161	0.242	0.374	0.401	0.482	0.546
	90	0.145	0.175	0.229	0.306	0.384	0.406
0.1	30	4.055	6.367	7.273	9.312	9.550	10.877
	60	2.526	3.589	5.110	5.240	6.122	6.847
	90	2.289	2.714	3.448	4.412	5.059	5.429
0.3	30	5.610	8.135	8.982	10.592	11.189	11.490
	60	3.911	5.267	6.898	7.093	8.075	8.555
	90	3.551	4.205	5.204	6.397	6.656	7.211
0.5	30	5.897	8.404	9.173	9.263	10.006	10.937
	60	4.210	5.598	6.914	7.159	7.532	8.199
	90	3.830	4.540	5.608	6.165	6.889	6.903

$$K_{3\alpha-1,3\beta-1} = \frac{E\phi h}{2(1+v)(1-2v)}\left[\frac{(1-v)}{\phi^2} C^{0,0}_{i,l} A^{1,1}_{j,m} A^{0,0}_{k,n} + \frac{(1-2v)}{2} B^{1,1}_{i,l} A^{0,0}_{j,m} A^{0,0}_{k,n} - \frac{(1-2v)}{2}(A^{1,0}_{i,l} A^{0,0}_{j,m} A^{0,0}_{k,n} + A^{0,1}_{i,l} A^{0,0}_{j,m} A^{0,0}_{k,n}) + \frac{(1-2v)}{2} C^{0,0}_{i,l} A^{0,0}_{j,m} A^{0,0}_{k,n} + \frac{2(1-2v)(b-a)^2}{h^2} B^{0,0}_{i,l} A^{0,0}_{j,m} A^{1,1}_{k,n}\right], \tag{A.5}$$

Table 8
Non-dimensional frequencies Ω for the 6 lowest modes of annular sector F-F-C-C plates ($a/b = 0.5$, $v = 0.3$)

h/b	ϕ (deg)	Mode no.					
		1	2	3	4	5	6
0.005	30	0.154	0.294	0.405	0.438	0.623	0.672
	60	0.042	0.105	0.109	0.206	0.208	0.232
	90	0.019	0.051	0.060	0.096	0.127	0.155
0.1	30	2.402	4.024	5.228	5.419	7.402	7.637
	60	0.770	1.716	1.845	3.203	3.215	3.487
	90	0.367	0.925	1.033	1.670	2.108	2.545
0.3	30	3.695	5.354	6.796	7.133	8.135	9.366
	60	1.592	2.748	3.161	4.955	5.159	5.345
	90	0.880	1.861	1.881	3.053	3.505	4.260
0.5	30	3.997	5.345	7.007	7.007	7.617	8.329
	60	1.889	2.854	3.450	5.227	5.367	5.438
	90	1.138	2.009	2.173	3.459	3.662	4.515

$$K_{3\alpha-1,3\beta} = \frac{E(b-a)}{(1+v)(1-2v)}\left[vA_{i,l}^{0,0}A_{j,m}^{1,0}A_{k,n}^{0,1} + \frac{(1-2v)}{2}A_{i,l}^{0,0}A_{j,m}^{0,1}A_{k,n}^{1,0}\right], \tag{A.6}$$

$$K_{3\alpha,3\beta-2} = \frac{E\phi}{(1+v)(1-2v)}\Big[v(b-a)B_{i,l}^{0,1}A_{j,m}^{0,0}A_{k,n}^{1,0} + (1-2v)(b-a) \times B_{i,l}^{1,0}A_{j,m}^{0,0}A_{k,n}^{0,1} + v(b-a)A_{i,l}^{0,0}A_{j,m}^{0,0}A_{k,n}^{1,0}\Big], \tag{A.7}$$

$$K_{3\alpha,3\beta-1} = \frac{E(b-a)}{(1+v)(1-2v)}\left[vA_{i,l}^{0,0}A_{j,m}^{0,1}A_{k,n}^{1,0} + \frac{(1-2v)}{2}A_{i,l}^{0,0}A_{j,m}^{1,0}A_{k,n}^{0,1}\right], \tag{A.8}$$

$$K_{3\alpha,3\beta} = \frac{E\phi h}{2(1+v)(1-2v)}\left[\frac{2(1-v)(b-a)^2}{h^2}B_{i,l}^{0,0}A_{j,m}^{0,0}A_{k,n}^{0,1} + \frac{(1-2v)}{2}B_{i,l}^{1,1}A_{j,m}^{0,0}A_{k,n}^{0,0} + \frac{(1-2v)}{2\phi^2}C_{i,l}^{0,0}A_{j,m}^{1,1}A_{k,n}^{0,0}\right], \tag{A.9}$$

$$M_{3\alpha-2,3\beta-2} = M_{3\alpha-1,3\beta-1} = M_{3\alpha,3\beta} = \tfrac{1}{2}\rho(b-a)^2\phi h B_{i,l}^{0,0}A_{j,m}^{0,0}A_{k,n}^{0,0}, \tag{A.10}$$

$$M_{3\alpha-2,3\beta-1} = M_{3\alpha-2,3\beta} = M_{3\alpha-1,3\beta} = M_{3\alpha-1,3\beta-2} = M_{3\alpha,3\beta-2} = M_{3\alpha,3\beta-2} = 0. \tag{A.11}$$

Appendix B. Nomenclature

a	inner radius
b	outer radius
h	thickness
ϕ	sector angle
r, θ, z	cylindrical co-ordinates
ξ, η, ζ	non-dimensional co-ordinates
u, v, w	displacements in the r, θ, z directions
L, M, N	numbers of hierarchical modes in the r, θ, z directions
ρ	mass density
E	modulus of elasticity
v	the Poisson ratio
$\mathbf{K}_{\alpha,\beta}$	stiffness matrix
$\mathbf{M}_{\alpha,\beta}$	mass matrix
ω	natural frequency
$\Omega = \omega b\sqrt{\rho/E}$	non-dimensional frequency

References

[1] T. Mizusawa, Vibration of thick annular sector plates using semi-analytical methods, *Journal of Sound and Vibration* 150 (1991) 245–259.
[2] M. Abramowitz, I.A. Stegun, Handbook of Mathematical Functions, Dover Publications, New York, 1965.